

## Custom 3d printer and resins for $18 \mu\text{m} \times 20 \mu\text{m}$ microfluidic flow channels

### S1 3D Printer

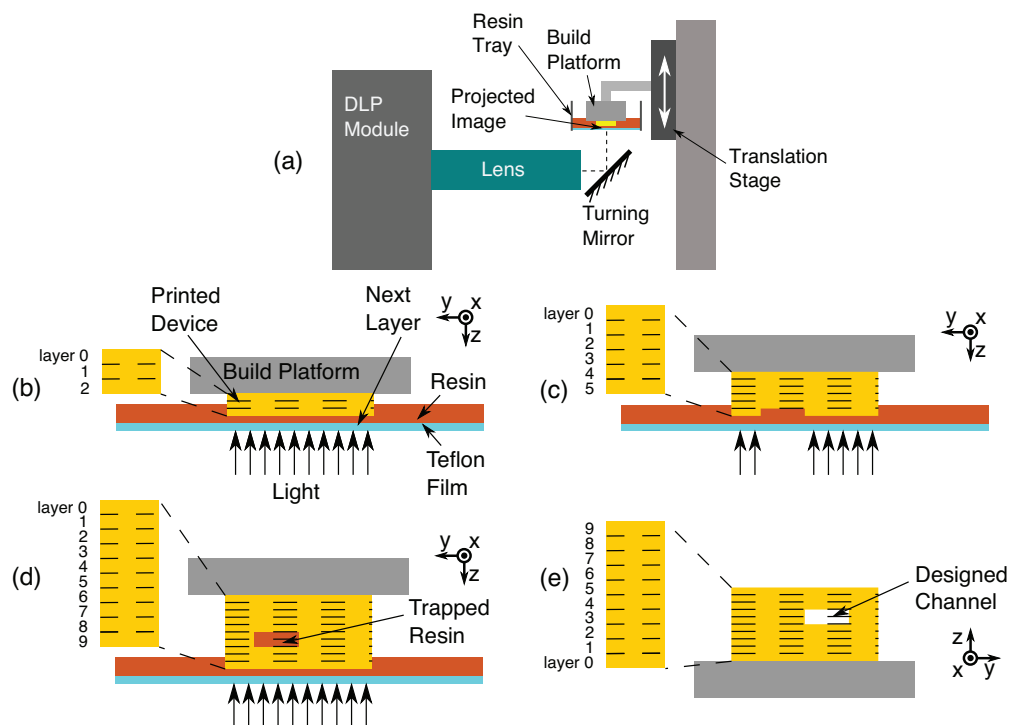


Figure S1: (a) Schematic illustration of 3D printer. (b)-(e) Process to 3D print a device, illustrating the formation of a microfluidic flow channel (i.e., void region).

Fig. S1(a) shows a schematic illustration of our 3D printer and the spatial relationship between the various components. During operation (Fig. S1(b)-(e)), a device is fabricated upside down with light incident through a transparent Teflon film which comprises the bottom of the resin tray. Each layer is formed by raising the build platform several millimeters to permit fresh resin to flow into the space between the Teflon film and the last built layer, followed by lowering the build platform such that the last built layer is separated from the Teflon film by  $z_l$ , the build layer thickness. The uncured resin in this space is then photopolymerized in the desired pattern by exposure to an image projected by the DLP module, lens system, and turning mirror.

We have done some preliminary characterization using SEM measurements for 2% NPS resin of the actual build layer thicknesses achieved by our system compared to the design thicknesses of 5, 7.5, 8.3, and  $10 \mu\text{m}$ . This analysis shows that the average measured build layer thickness is 7.6% smaller than the designed thickness with a standard deviation of 7.5%. A few initial measurements for the 3% NPS resin design thicknesses of 6 and  $7 \mu\text{m}$  show measured thicknesses that are 12% smaller. While better build layer thickness fidelity can likely be achieved by replacing the stock Solus z-translation mechanism with one having higher performance, we have found the stock mechanism to be sufficient for the purposes of this paper in which we demonstrate how to achieve  $18 \mu\text{m} \times 20 \mu\text{m}$  3D printed flow channels.

## S2 Molecular structures

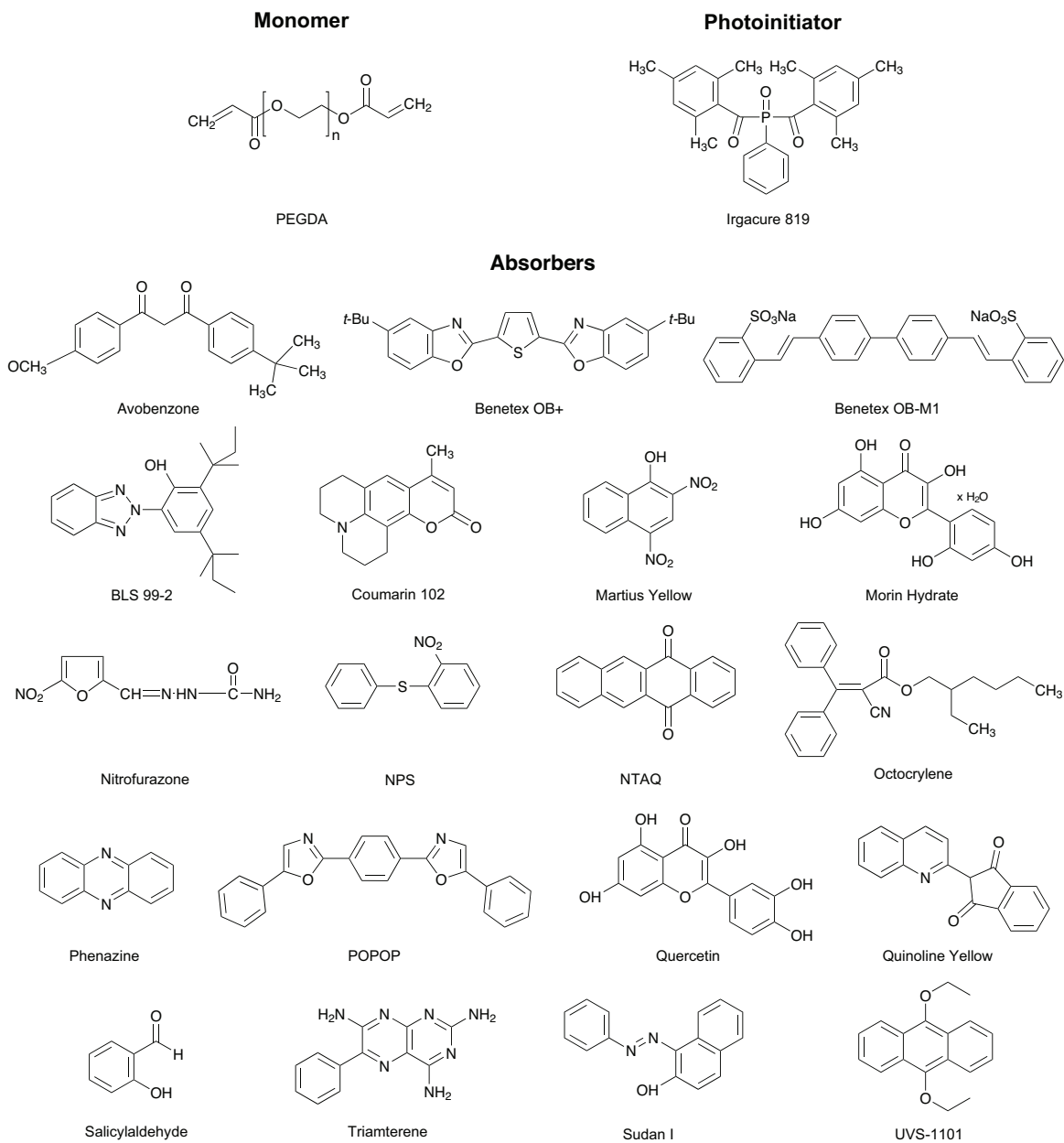


Figure S2: Molecular structures for monomer, photoinitiator, and UV absorbers used in this study (except for UV386A, which is proprietary).

Table S1: Comparison of monochromatic and polychromatic resin exposures

Line	Parameter	Units	Symbol	Monochromatic Case	Polychromatic Case
1	Irradiance at $z = 0$	W/cm <sup>2</sup>	$I_0$	$I_0$	$\int_0^\infty I_0(\lambda) d\lambda$
2	Irradiance as a function of $z$	W/cm <sup>2</sup>	$I(z)$	$I_0 e^{-\alpha z}$	$\int_0^\infty I_0(\lambda) e^{-\alpha(\lambda)z} d\lambda$
3	Dose as a function of $z, t$	J/cm <sup>2</sup>	$D(z, t)$	$t I_0 e^{-\alpha z}$	$t \int_0^\infty I_0(\lambda) e^{-\alpha(\lambda)z} d\lambda$
4	Critical dose	J/cm <sup>2</sup>	$D_c$	$t_p I_0 e^{-z_p/h_a}$	$t_p \int_0^\infty I_0(\lambda) e^{-\alpha(\lambda)z_p} d\lambda$
5	Time to reach critical dose at $z = 0$	s	$T_c$	$D_c/I_0$	$D_c/\int_0^\infty I_0(\lambda) d\lambda$
6	Polymerization depth	$\mu\text{m}$	$z_p$	$h_a \ln \frac{t_p}{T_c}$	see below

### S3 Monochromatic and polychromatic resin exposure comparison

Table S1 summarizes the parameters that are important for monochromatic exposure of photopolymerizable resins as defined in Ref. 1. It also gives the corresponding expressions for polychromatic resin exposures so the two cases can be directly compared.

### S4 Derivation of Model 4

The critical dose,  $D_c$ , on Line 4 in Table S1 is the dose required to just polymerize a resin for a given irradiance. This dose occurs at the leading edge of the polymerization thickness,  $z_p$ , which corresponds to a specific polymerization time,  $t_p$ . *For the monochromatic case* we can solve Line 4 for the polymerization time (using Line 5) as

$$\frac{t_p}{T_c} = e^{z_p/h_a}, \quad (\text{S1})$$

which leads to Eq. 1 for  $z_p$  in the main text (Model 3, which is also on Line 6).

*For the polychromatic case* we cannot obtain an analytic expression for the polymerization depth,  $z_p$ . Instead, we must solve for  $t_p$ . Beginning with Line 5,

$$T_c = \frac{D_c}{\int_0^\infty I_0(\lambda) d\lambda}, \quad (\text{S2})$$

and substituting for  $D_c$  (Line 4), we obtain

$$\frac{T_c}{t_p} = \frac{\int_0^\infty I_0(\lambda) e^{-\alpha(\lambda)z_p} d\lambda}{\int_0^\infty I_0(\lambda) d\lambda} \quad (\text{S3})$$

$$= D_n(z_p) \quad (\text{S4})$$

$$\approx (1 - a) + a \exp(-z_p/b) \quad (\text{S5})$$

where  $D_n(z)$  is the normalized dose defined in Eq. 3 and Eq. S5 is from Eq. 6 in the main text. Solving for  $t_p$  we obtain

$$t_p = \frac{T_c}{(1 - a) + a \exp(-z_p/b)}, \quad (\text{S6})$$

which is Model 4.

Table S2: Summary of fit parameters based on measured spectra and on measured thickness vs. exposure time data. All resins are formulated with 1% Irgacure 819 in addition to the specified absorber.

Material	Solubility	Concentration	Fit from measured spectrum			Fit from measured thickness vs. exposure time				
			Model 1	Model 2		Model 3		Model 4		
			$h_a$ ( $\mu\text{m}$ )	$a$	$b$ ( $\mu\text{m}$ )	$h_a$ ( $\mu\text{m}$ )	$T_c$ (ms)	$a$	$b$ ( $\mu\text{m}$ )	$T_c$ (ms)
<b>Photoinitiator</b>										
Irgacure 819	>5%	1%	218.85	0.98	208.47	196.13	89.42	1.00	193.40	88.21
<b>UV Absorbers</b>										
Avobenzone	>5%	1%	15.10	0.92	10.70	20.00	283.23	0.84	10.49	258.93
Benetex OB+	0.25%	0.25%	19.15	0.97	17.50	24.47	56.37	0.98	21.65	55.95
BLS 99-2	>5%	2%	57.28	0.97	50.65	72.49	202.13	0.92	51.30	181.92
Coumarin 102	0.8%	0.5%	11.98	0.97	11.03	19.55	123.59	0.95	12.00	90.90
Martius Yellow	3%	1%	15.26	0.98	14.34	13.28	448.69	1.00	13.03	423.74
NPS	>5%	2%	11.74	0.98	11.17	11.18	307.33	1.00	10.88	280.44
NPS		3%	8.28	0.99	7.94	8.05	413.72	1.00	8.16	427.58
Octocrylene	>5%	1%	194.96	0.98	184.13	173.84	95.75	1.00	173.00	95.27
Phenazine	1.8%	0.5%	33.47	0.97	30.30	23.03	1005.38	0.96	19.51	936.94
Quercetin	0.8%	0.5%	16.16	0.96	14.12	12.03	324.96	1.00	12.18	333.04
Salicylaldehyde	>5%	2%	175.21	0.98	166.75	162.94	90.05	1.00	164.19	90.58
Sudan I	2.7%	0.6%	18.08	1.00	17.99	16.92	335.62	1.00	14.95	227.14
UVS-1101	0.5%	0.5%	31.20	0.98	28.92	34.03	105.75	0.96	24.11	78.80

## S5 Fits to Models 1–4

As seen in Table S2, absorbers with good spectral overlap with the source spectrum as observed in Fig. 3(a) have fits to Model 2 in which  $a \approx 1$ . In this case Model 2 reduces to Model 1 and the corresponding fits for  $b$  and  $h_a$  are in reasonable agreement. Likewise, when Models 3 and 4 are fit to experimental thickness versus exposure data, good spectral overlap corresponds to  $a = 1$  in Model 4 such that Model 4 reduces to Model 3 and  $b$  and  $h_a$  are fairly consistent with not only each other, but also with  $b$  and  $h_a$  obtained solely from the measured molar absorptivity in Models 1 and 2. An important ramification is that for absorbers with good spectral overlap with the source it is unnecessary to experimentally measure the thickness as a function of exposure to determine  $h_a$ . Instead,  $h_a$  can be found by using it as a fitting parameter in Eq. 7 in the main text where the absorption coefficient in  $D_n(z)$  is

$$\alpha(z) = \alpha_{abs}(\lambda) + \alpha_{pi}(\lambda) \quad (\text{S7})$$

where  $\alpha_{abs}(\lambda)$  and  $\alpha_{pi}(\lambda)$  are the absorber and photoinitiator absorption coefficients, respectively, calculated from their molar absorptivities.

## References

- [1] H. Gong, M. Beauchamp, S. Perry, A. T. Woolley and G. P. Nordin, *RSC Adv.*, 2015, **5**, 106621–106632.